Neuron, Volume *110*

Supplemental information

Edinger-Westphal peptidergic neurons enable maternal preparatory nesting

Thomas Topilko, Silvina L. Diaz, Catarina M. Pacheco, Florine Verny, Charly V. Rousseau, Christoph Kirst, Charlotte Deleuze, Patricia Gaspar, and Nicolas Renier

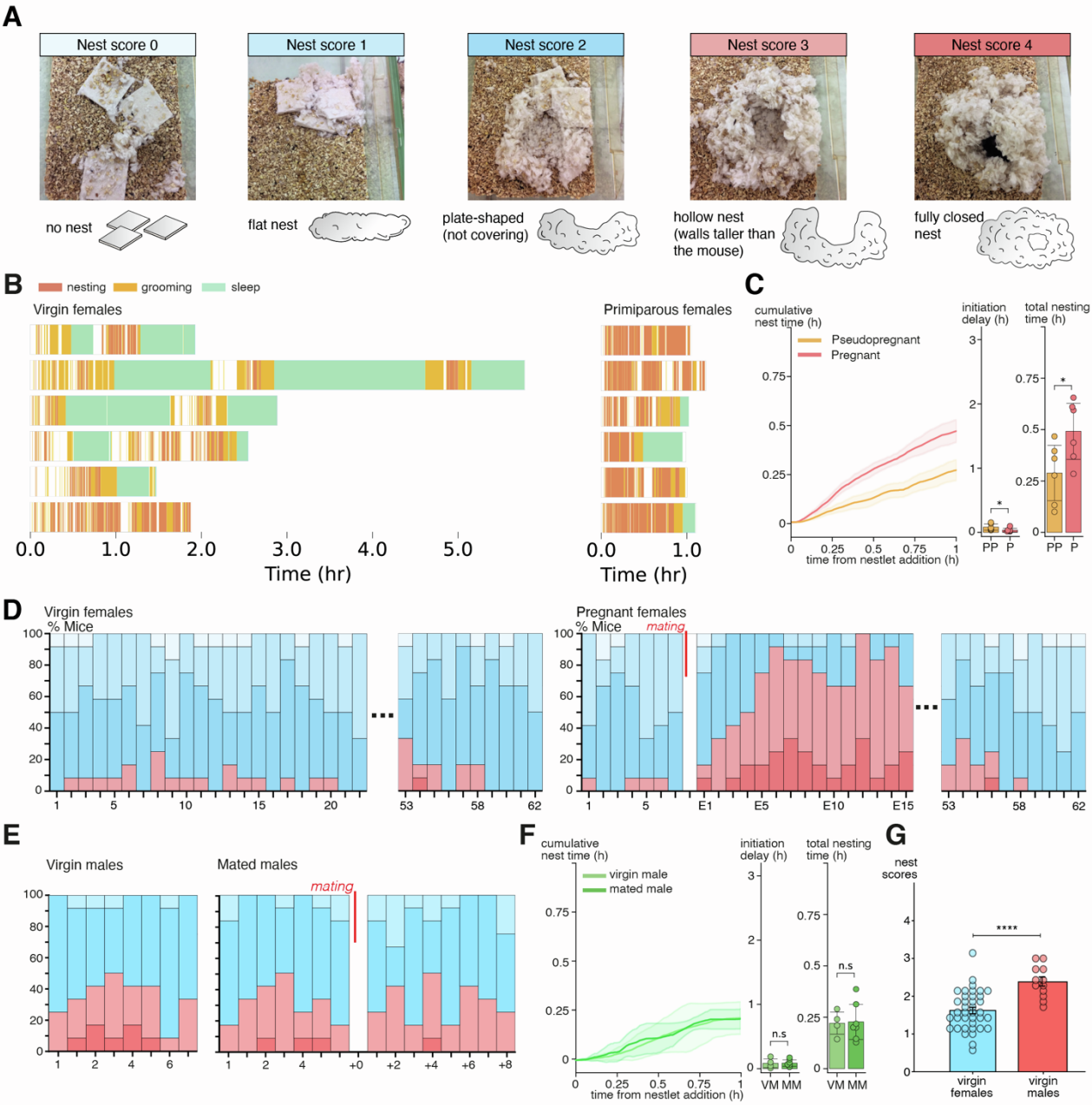
A
Nest score 0
Nest score 1
Nest score 2
Nest score 3
Nest score 4
no nest
flat nest
plate-shaped (not covering)
hollow nest (walls taller than the mouse)
fully closed nest
B
nesting
grooming
sleep
Virgin females
Primiparous females
0.0
1.0
2.0
3.0
4.0
5.0
Time (hr)
C
cumulative nest time (h)
Pseudopregnant
Pregnant
time from nestlet addition (h)
initiation delay (h)
total nesting time (h)
PP
P
D
Virgin females
% Mice
Pregnant females
mating
E
Virgin males
Mated males
mating
F
cumulative nest time (h)
virgin male
mated male
time from nestlet addition (h)
initiation delay (h)
total nesting time (h)
n.s
VM
MM
G
nest scores
****
virgin females
virgin males

Supplementary Figure 1, related to Figure 1. Characteristics of nest building in the mouse

(A) Photographs of nests viewed from the top, and their associated scores. Cartoons indicate how a cross-section through the nest would appear. Preparatory "brooding" nests (scores 3 and 4) are high enough to fully cover the mouse.

(B) Full event plot, related to figure 1D, of the mouse behavior following nestlets addition. The recordings were allowed to run until 1h after the initiation of the first major nesting event.

(C) Comparison of nesting activity over 1h in pregnant and pseudopregnant females at E15. Pseudopregnant females have a strong nesting capacity, but spend slightly less time nesting at E15 than pregnant females.

(D) long-term evolution of nesting through pregnancy and after weaning in a cohort of mice. After the weaning of the litter, nesting scores return to their baseline in primiparous females.

(E) Nesting scores in males are on average higher than in virgin females, but mating doesn't induce preparatory nesting in males.

(F) Segmentation of male nesting behavior before and after mating during 1h at the onset of the light phase, showing no effect of mating on the cumulative time spent nesting.

(G) Comparison of nest scores in virgin females and males, showing a higher baseline in virgin males.

Significance levels indicated are as follows: * $P < 0.05$, ** $P < 0.01$, *** $P < 0.001$ and **** $P < 0.0001$. All data are presented as mean ± SEM. Unpaired Mann-Whitney ranked U test (C, F-G).

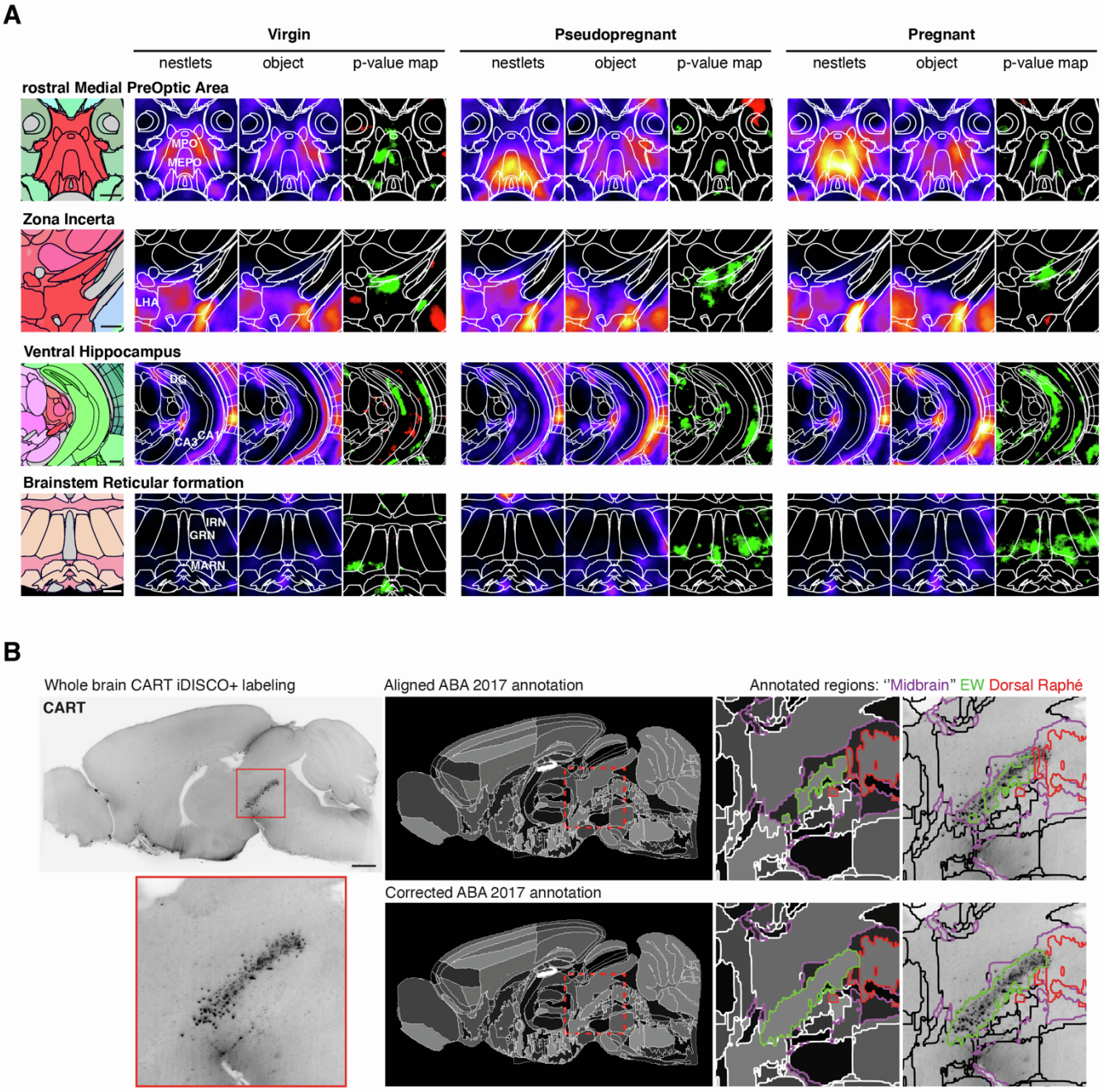

Supplementary Figure 2, related to Figure 2. Brain regions activated by nesting in all experimental groups.

(A) Heat maps of average registered Fos+ cells densities in virgin, pseudopregnant and pregnant females exposed to nestlets or control objects. The coronal views are shown at the levels of the rostral pro-optic areas, the zona incerta, the ventral hippocampus and the reticular formation. Unlike in the Edinger Westphal (Figure 2), these levels show regions induced by nesting in all groups.

Scale bars are 500µm.

(B) Modification of the Allen Brain Atlas annotation to better capture the full extent of the EW nucleus, based on aligned CART 3d datasets on the reference template. Scale bar is 1mm.

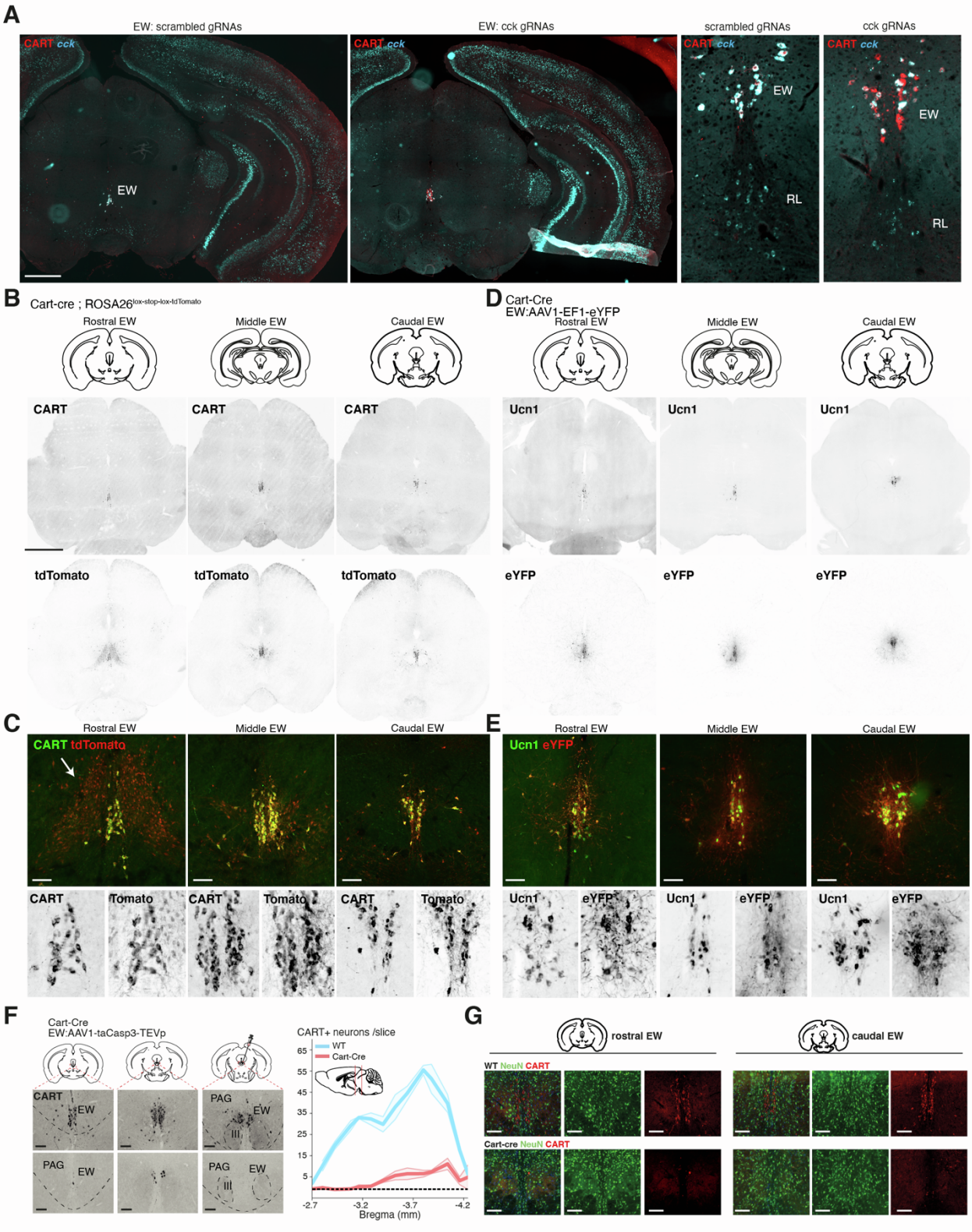
A
EW: scrambled gRNAs
EW: cck gRNAs
scrambled gRNAs
cck gRNAs
CART cck
EW
RL
B
Cart-cre ; ROSA26lox-stop-lox-tdTomato
Rostral EW
Middle EW
Caudal EW
CART
tdTomato
D
Cart-Cre
EW:AAV1-EF1-eYFP
Ucn1
eYFP
C
CART tdTomato
Tomato
E
Ucn1 eYFP
F
Cart-Cre
EW:AAV1-taCasp3-TEVp
PAG
III
CART+ neurons /slice
WT
Cart-Cre
Bregma (mm)
G
rostral EW
caudal EW
WT NeuN CART
Cart-cre NeuN CART

Supplementary Figure 3, related to Figure 5 Validation of the EWcp^{CART+} targeting and neuronal ablation.

(A) Slices of adult mouse brains injected with scrambled CRISPR AAVs or CCK gRNAs AAVs, at the level of the rostral EW (left) and caudal EW (right), hybridized for CCK and immunolabeled for CART. The magnified panels show CCK+ neurons of the Rostral Linear Raphe (RL), ventral to the EWcp neurons. The expression of CCK is not noticeably reduced outside of the EW region, but the RL nucleus shows a small reductions in the number of CCK+ cells as well.

(B,C) Sections at the level of the rostral, middle or caudal EW nucleus of Cart-Cre ; Rosa26-lsl-tdTomato adult mice, immunolabeled for tdTomato and CART. The sections show perfect overlap between CART and tdTomato in the EW, but also leaky tdTomato expression in the rostral Ew (arrow).

(D,E) Sections at the level of the rostral, middle or caudal EW nucleus of Cart-Cre mice injected with a eYFP expressing AAV1, and immunolabeled for eYFP and Ucn1, showing perfect overlap between the eYFP+ cells and the Ucn1+ cells. Of note, the neurons expressing tdTomato outside the EW nucleus (see C) do not express eYFP.

(F) The ablation of CART+ neurons of the EW is efficient along the full rostro-caudal axis of the nucleus.

(**G)** Sections at rostral and caudal levels of the EW nucleus of WT and Cart-Cre animals injected with the activated Caspase 3 AAV, 2 weeks after injection, immunolabeled for CART and NeuN. No alteration of the density of NeuN neurons in the EW region is visible in the ablated animals.

Scale bars are 1mm (A-D) or 150µm (C-G).

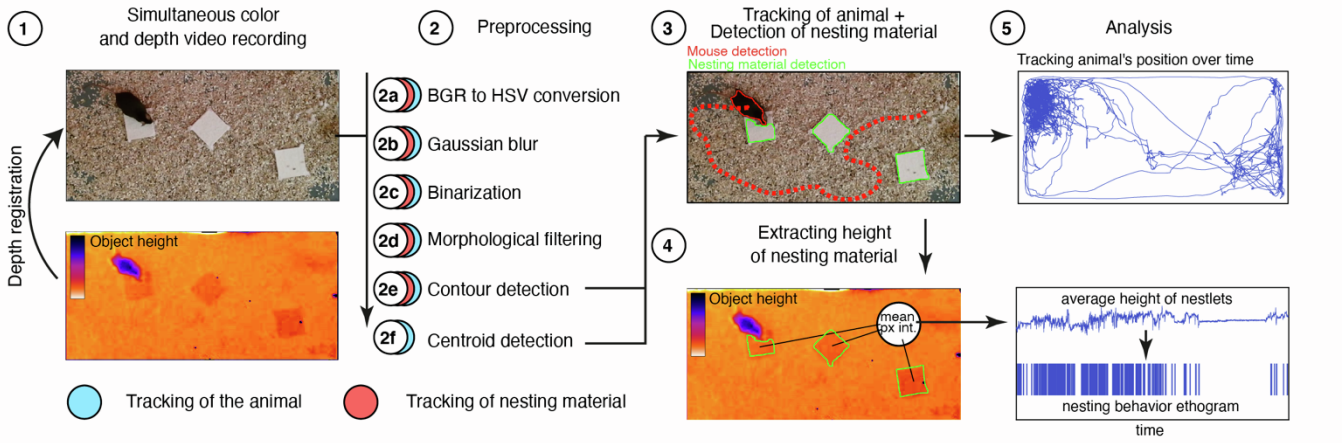

Supplementary Figure 4, related to Figure 5. Automated video tracking system for nest building.

Open field behaviors are recorded with a Kinect camera (Microsoft). Both Infrared and RGB channels are registered, and a set of filters is applied to track both the mouse and the nestlets based on their colors. The cumulative height of nestlets is then evaluated. Variations in height are then interpreted as interaction events.

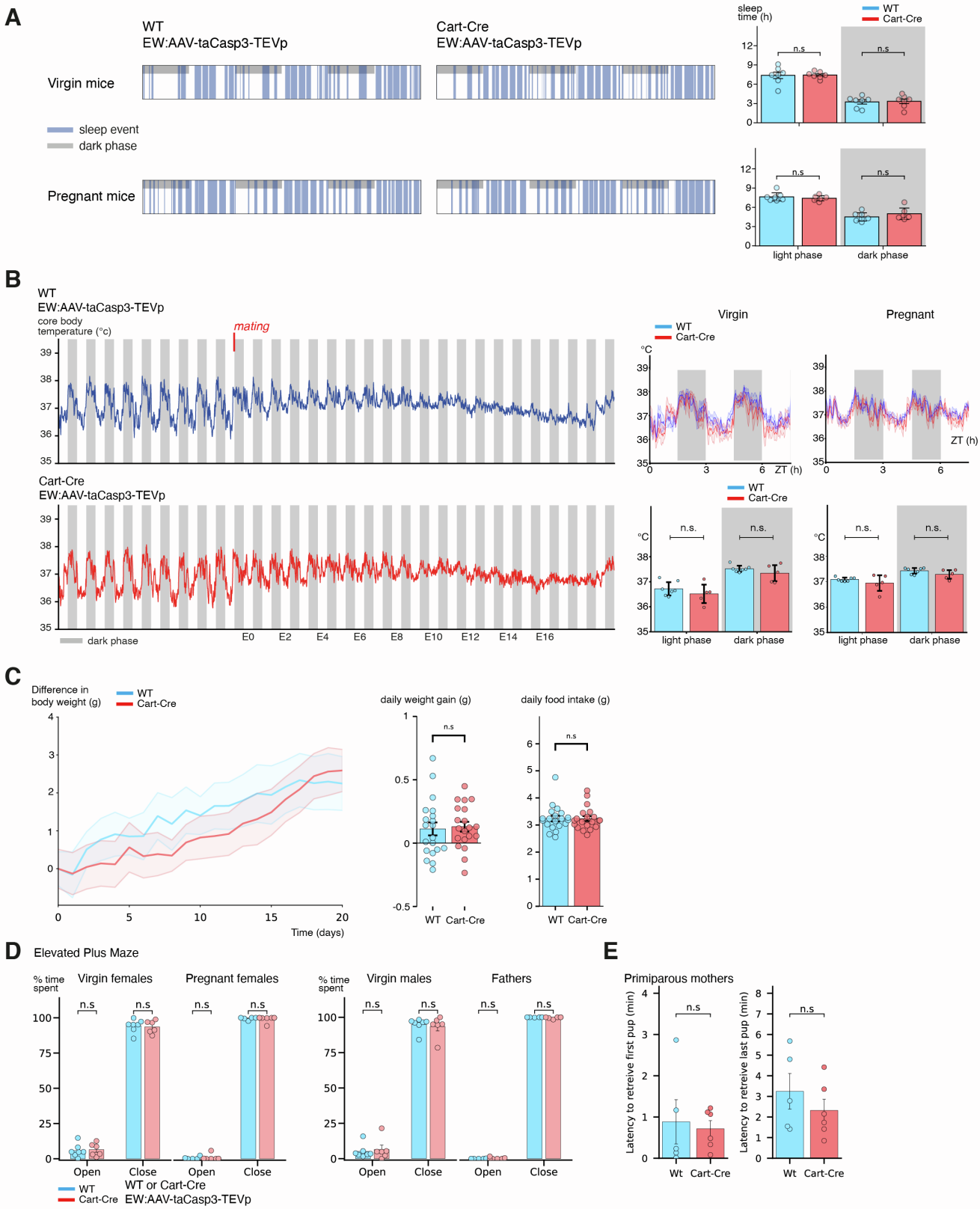
A
WT
EW:AAV-taCasp3-TEVp
Cart-Cre
EW:AAV-taCasp3-TEVp
Virgin mice
sleep event
dark phase
Pregnant mice
sleep time (h)
WT
Cart-Cre
n.s
light phase
dark phase
B
WT
EW:AAV-taCasp3-TEVp
core body temperature (°c)
mating
Cart-Cre
EW:AAV-taCasp3-TEVp
dark phase
E0 E2 E4 E6 E8 E10 E12 E14 E16
Virgin
Pregnant
ZT (h)
°C
n.s.
C
Difference in body weight (g)
Time (days)
daily weight gain (g)
daily food intake (g)
D
Elevated Plus Maze
% time spent
Virgin females
Pregnant females
Virgin males
Fathers
Open
Close
WT or Cart-Cre
EW:AAV-taCasp3-TEVp
E
Primiparous mothers
Latency to retreive first pup (min)
Latency to retreive last pup (min)
Wt
Cart-Cre

Supplementary Figure 5, related to Figure 5. Absence of long-term physiological effects of the EWcp^{CART+} neuronal ablation.

(A) Video tracking of sleep over 3 days in control and ablated animals. Changes in the duration of the sleep bouts are visible between the light and dark phases in both control and ablated female animals, but no significant changes in the sleep bout patterns are measured between both groups, in virgin or pregnant animals.

(**B)** Evolution of the core body temperature during gestation in control and ablated female animals. Regulation of the core body temperature is visible on the day following mating in both groups. No significant differences are recorded between both groups, in virgin or pregnant animals.

(**C**) Evolution of daily body weight gain and food intake in virgin WT and Cart-Cre mice injected with the taCasp3-tevp AAV over 3 weeks.

(D) Time spent in the open and closed arms of an Elevated "Plus" Maze for virgin and pregnant females, virgin or parental males, in control or EWcp^{CART+}-ablated mice, showing no effect of the ablation on this behavior.

(E) Time to retrieve pups primiparous control or EWcp^{CART+}-ablated mothers. No difference is recorded between the groups.

Significance levels indicated are as follows: * $P < 0.05$, ** $P < 0.01$, *** $P < 0.001$ and **** $P < 0.0001$. All data are presented as mean ± SEM. Unpaired Mann-Whitney ranked U test (A-E).

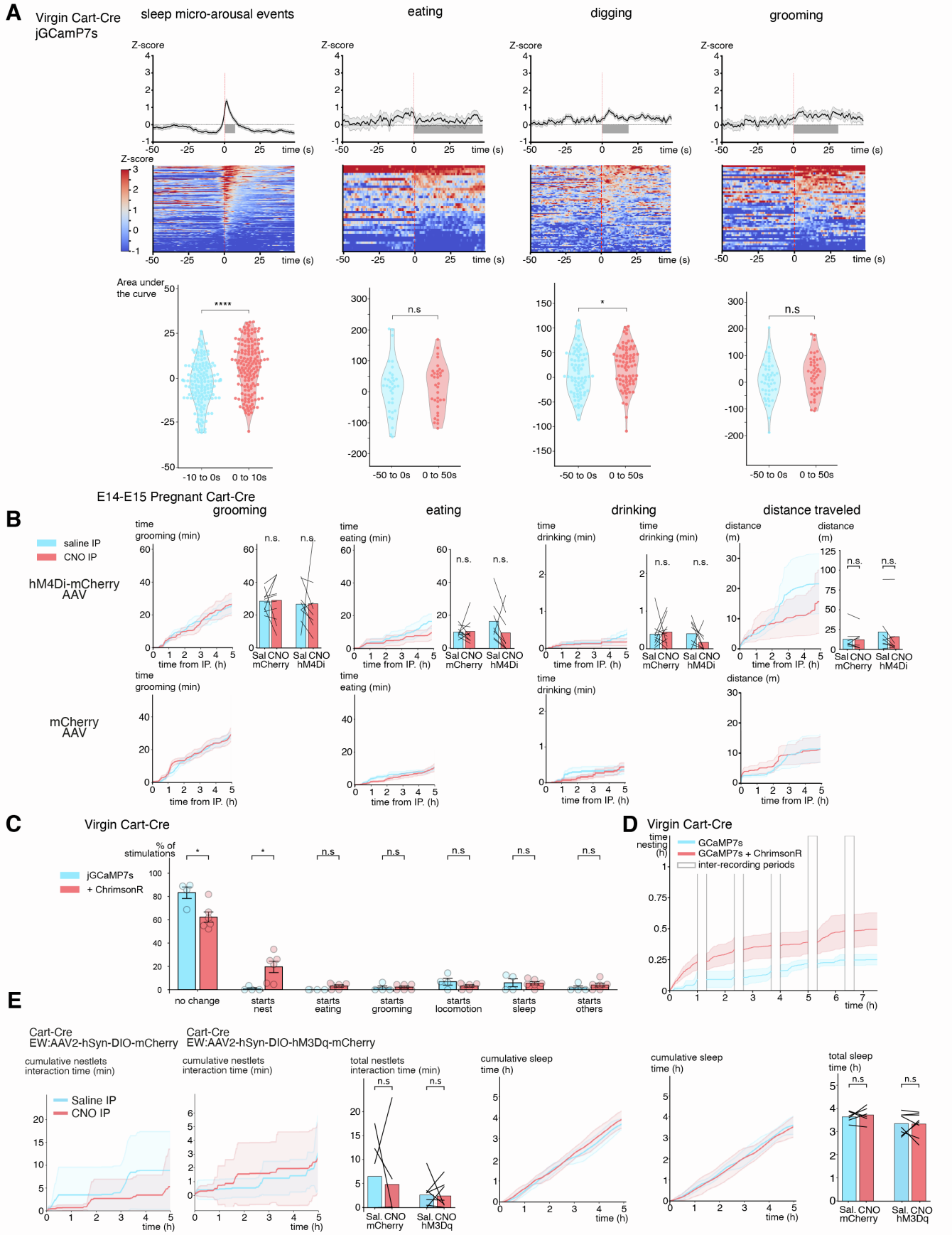
A
Virgin Cart-Cre
jGCamP7s
sleep micro-arousal events
eating
digging
grooming
Z-score
time (s)
Area under the curve
****
n.s
*
-10 to 0s
0 to 10s
-50 to 0s
0 to 50s
B
E14-E15 Pregnant Cart-Cre
grooming
eating
drinking
distance traveled
saline IP
CNO IP
hM4Di-mCherry AAV
mCherry AAV
time grooming (min)
time eating (min)
time drinking (min)
distance (m)
time from IP. (h)
n.s.
Sal CNO mCherry
Sal CNO hM4Di
C
Virgin Cart-Cre
jGCaMP7s
+ ChrimsonR
% of stimulations
n.s
no change
starts nest
starts eating
starts grooming
starts locomotion
starts sleep
starts others
D
Virgin Cart-Cre
time nesting (h)
GCaMP7s
GCaMP7s + ChrimsonR
inter-recording periods
time (h)
E
Cart-Cre
EW:AAV2-hSyn-DIO-mCherry
Cart-Cre
EW:AAV2-hSyn-DIO-hM3Dq-mCherry
cumulative nestlets interaction time (min)
total nestlets interaction time (min)
cumulative sleep time (h)
total sleep time (h)
Saline IP
CNO IP
Sal. CNO mCherry
Sal. CNO hM3Dq

Supplementary Figure 6, related to Figure 6. Behavioral specificity of activity, inhibition and activation of EWcpCART+ neurons towards nesting.

(A) Peri-event plots of fiber photometry recordings in virgin Cart-Cre females, implanted at the level of the EW and injected with a jGCaMP7s-expressing AAV. Strong calcium signal is recorded during micro-arousal events during sleep (determined by muscular twitches from the video recordings). No significant changes in the Z-scores are measured during eating, digging or grooming.

(**B)** Cumulative curves of behaviors over 5h during the light phase in E14-E15 pregnant females injected with an AAV expressing hM4Di and mCherry, or mCherry alone, injected with saline and CNO at the beginning of the light phase. No significant changes are seen between the saline and CNO injections on the time spend grooming, eating or drinking, nor on the total distance traveled.

(**C)** Effect of the optogenetic stimulation regimen (see Figure 4H) on different behavioral transitions in virgin Cart-Cre mice injected with AAVs expressing jGCaMP7s or jGCaMP7s and ChrimsonR. No significant increase in eating, grooming, locomotion start or sleep are measured in the ChrimsonR-injected mice, while a significant increase in the proportion of stimulations eliciting nesting is measured.

(D) Cumulative nesting times for virgin mice injected with jGCaMP7s alone or GCaMP7s and ChrimsonR following the stimulation regimen detailed in figure 5H. The white bars indicate the 20min inter-stimulation times, during which no recording is made. Stimulations made during early recording sessions are more effective than those made after the beginning of the light phase (second half of the graph, from 3.5h).

(**E**) Virgin Cart-Cre mice are injected with an AAV expressing hM3Dq and mCherry. Cumulative curves of time spent interacting with nestlets or sleeping over a 5h period during the light phase, following either saline or CNO injections at the beginning of the light phase. No differences are measured between the CNO or saline injected groups.

Significance levels indicated are as follows: * $P < 0.05$, ** $P < 0.01$, *** $P < 0.001$ and **** $P < 0.0001$. All data are presented as mean ± SEM. Unpaired Mann-Whitney ranked U test (C) and Wilcoxon's signed rank test (A,B,E).

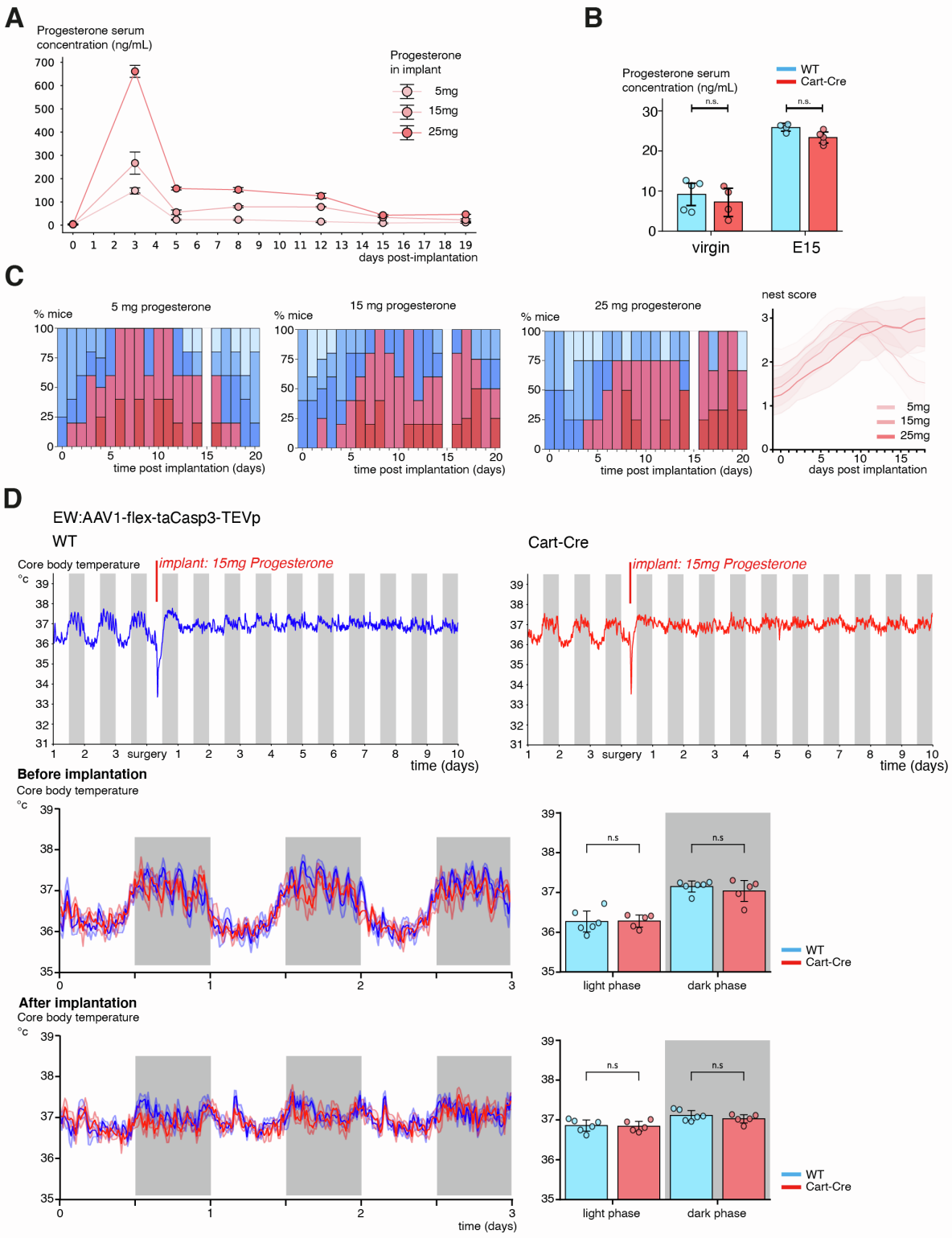
A
Progesterone serum concentration (ng/mL)
Progesterone in implant
5mg
15mg
25mg
days post-implantation
B
Progesterone serum concentration (ng/mL)
WT
Cart-Cre
n.s.
virgin
E15
C
5 mg progesterone
15 mg progesterone
25 mg progesterone
% mice
time post implantation (days)
nest score
days post implantation
D
EW:AAV1-flex-taCasp3-TEVp
WT
Cart-Cre
Core body temperature
°c
implant: 15mg Progesterone
surgery
time (days)
Before implantation
After implantation
light phase
dark phase
n.s

Supplementary Figure 7, related to Figure 7. Role of the progesterone on preparatory nesting.

(A) Measure of the circulating progesterone in virgin and E15 pregnant control and EW-ablated female mice. The absence of the EWcp CART+ neurons doesn't affect the circulating progesterone serum concentrations at these stages. We measured during pregnancy progesterone levels ranging from 9.2±1.7 (E1) to 25.9±1.0 (E15).

(**B)** Effect of sub-cutaneous implants of various sizes on circulating progesterone concentrations over time. Implants of 5, 15, and 25mg raised the level of circulating progesterone from 4.0±0.6 ng/mL to a peak of 148.6±8.6, 267.0±33.6, 661.2±18.3 ng/mL respectively, with a plateau of 23.6±0.1, 79.2±33.6 and 152.4±9.1 ng/mL respectively 8 days after implantation.

(**C)** Effect of sub-cutaneous implants of various sizes on nest scores over time.

(**D)** Effect of sub-cutaneous implants of 15mg on core-body temperature in control or Cart-Cre EW ablated mice. In both groups, the presence of the implant modulates the core body temperature the day following implantation onwards, and no differences in the response to the implant is seen between the groups.

Significance levels indicated are as follows: * $P < 0.05$, ** $P < 0.01$, *** $P < 0.001$ and **** $P < 0.0001$. All data are presented as mean ± SEM. Unpaired Mann-Whitney ranked U test (D).

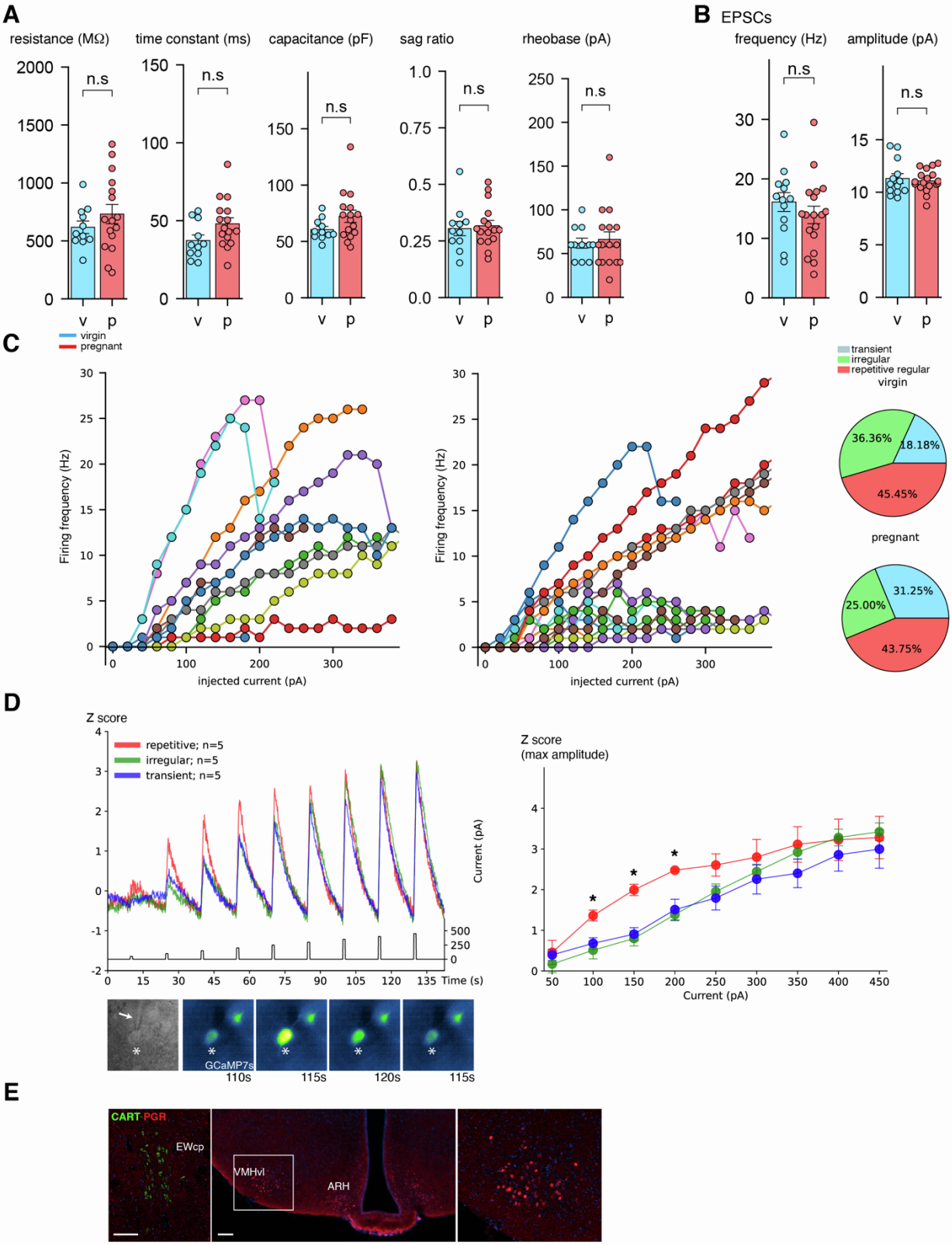
A
resistance (MΩ)
time constant (ms)
capacitance (pF)
sag ratio
rheobase (pA)
n.s
v
p
virgin
pregnant
B
EPSCs
frequency (Hz)
amplitude (pA)
C
Firing frequency (Hz)
injected current (pA)
transient
irregular
repetitive regular
virgin
36.36%
18.18%
45.45%
pregnant
31.25%
25.00%
43.75%
D
Z score
repetitive; n=5
irregular; n=5
transient; n=5
Current (pA)
Time (s)
GCaMP7s
110s
115s
120s
115s
Z score
(max amplitude)
Current (pA)
E
CART PGR
EWcp
VMHvl
ARH

Supplementary Figure 8, related to Figure 7. Intrinsic properties of the EWcp neurons.

(A) Intrinsic and (**B**) synaptic electrophysiological properties of the recorded EWcp^{CART+} neurons, obtained from patch recordings. Slices obtained from virgin and pregnant females were obtained and compared. No significant differences are measured in the considered properties between virgin and pregnant females.

(**C**) Summary of the input-output relationship of the evoked firing for individual cells, and changes in the ratio of the related firing pattern during pregnancy. A smaller proportion of irregular cells with a larger proportion of transient-firing cells are recorded in slices obtained from pregnant females.

(D) Patch recordings of EWcp^{CART+} neurons in acute slices obtained from virgin *Cart-Cre* mice injected with an AAV carrying jGCaMP7s. The calcium-dependent fluorescence was recorded during current injections of increasing amplitude. The calcium transients were then sorted according to the firing mode of the neuron, as defined in Figure 6E. While the amplitude of the calcium transients was similar across the different neuron types, there was a significant increase in the amplitude of the calcium transient for smaller current injections in repetitive neurons compared to irregular and transient neurons.

(E) Brain sections of a E15 pregnant female mouse at the level of the EW and Arcuate Nucleus of the Hypothalamus (ARH), immunolabeled for CART and Progesterone nuclear Receptor (PGR). PGR is not detected in the EW, while positive cells are seen in the VentroMedial nucleus of the Hypothalamus (VMHvl) and ARH. Scale bars are 150µm.

Significance levels indicated are as follows: * $P < 0.05$, ** $P < 0.01$, *** $P < 0.001$ and **** $P < 0.0001$. All data are presented as mean ± SEM. Unpaired Mann-Whitney ranked U test (A,B,D).